SYNERGY OF RADAR AND OPTICAL IMAGES FOR VEGETATION DAMAGE ASSESSMENT OF SUPER TYPHOON RAI IN SEVERELY AFFECTED AREAS OF CARAGA REGION, PHILIPPINES

Jonel G. Vernante[1,2], Kendel P. Bolanio[1,2], Monalaine M. Bermoy[1,2], Arnaldo C. Gagula[1,2], Rey Joshua C. Jaque[1], Donna Mae T. Labaso[1]

[1]Department of Geodetic Engineering, Caraga State University, Ampayon, Butuan City 8600, Philippines
Emails: reyjoshua.jaque@carsu.edu.ph, donnamae.labaso@carsu.edu.ph

[2]Caraga Center for Geo-informatics, Caraga State University, Ampayon, Butuan City 8600, Philippines
Emails: jgvernante@carsu.edu.ph, kpbolanio@carsu.edu.ph, mmbermoy@carsu.edu.ph, acgagula@carsu.edu.ph

KEY WORDS: Vegetation damage assessment, coherence change detection (CCD), NDVI, Typhoon Rai

ABSTRACT: On the 16th of December 2021, a Category 5 Typhoon Rai made landfall in the Philippines. Events like these require an assessment of the damages to vegetation which is usually done by comparing optical images before and after the disaster. The problem with using optical imagery alone is the lack of available data, especially on areas that experience extreme seasonal variations. Unlike optical imagery, Synthetic Aperture Radar (SAR) imagery uses active sensors, which can provide useful information even in bad weather and lacking illumination. This study employed a Coherence Change Detection using Sentinel-1 SAR imagery which compares two satellite radar photographs of one geographic area taken at different times to detect and measure changes in that area. Coherence change images were generated, showing areas of severe change to no change in four study areas. These sites include Dinagat Islands, Surigao city, Siargao Islands, and Bucas Grande, which were heavily impacted by the typhoon. Since vegetation has a short temporal decorrelation, which can cause false positives in the coherence change images, NDVI images for pre- and post-typhoon were generated to validate the output of CCD as typhoon-induced vegetation damages. While temporal decorrelation exhibits a general coherence loss over time, spontaneous decoherence after a disaster can be indicative of the damages.

1. INTRODUCTION

One of the country's relief responses to disasters like Typhoon Rai and an important component in rehabilitation efforts is the generation of damage assessment maps used to monitor and assess the impact caused by the typhoon. This is traditionally done through field surveying, which is made difficult by the restrictions due to COVID-19. The lack of accurate information is challenging regarding quick and effective emergency responses, which are critical for minimizing human losses and other casualties. In recent years, several modern Earth Observation (EO) systems continuously provide a massive amount of satellite data for free, making it possible to monitor the earth's surface without conducting in situ surveys. Remote sensing has significantly affected how impact assessments are done, making mapping at large-scales be cost-effective and easily repeatable. Satellite imagery is frequently used to assess vegetation damage because it can cover large geographic areas and has a high temporal range. A notable example is the Copernicus program developed by the European Space Agency (ESA), consisting of several Sentinel missions which monitor different aspects of the earth's surface.

The researchers present an approach of using Sentinel-1 Interferometric Synthetic Aperture Radar (InSAR) to assess the impact of typhoon Rai using the Coherence Change-Detection method (CCD). Unlike optical imagery, which uses passive sensors and is affected by bad weather conditions, SAR imagery uses active sensors to provide useful information even in bad weather and lacks illumination (Dong et al., 2011). The CCD compared the two coherence images, which then detected and measured the changes in the area. Because vegetation in nature is dynamic, the output of the CCD alone cannot quantify the damage because of the large possibility of false alarms. To increase the accuracy of the damage assessment, a Normalized Difference Vegetation Index (NDVI) change detection was used to validate the CCD results by correlating them to the output from the CCD. The researchers implemented this method in the areas of Dinagat Islands, Surigao City, Siargao Islands, and Bucas Grande (Figure 1) since they are geographically located along the typhoon path.

For this study, the researchers present a complete discussion of the methodology, which includes (i) generating a Coherence Change Image through CCD using pre- and post-typhoon Sentinel-1 SAR imagery, (ii) generating NDVI images using Landsat 8-9 optical images; and (iii) validating the coherence change image using visual inspection to compare with NDVI Images.

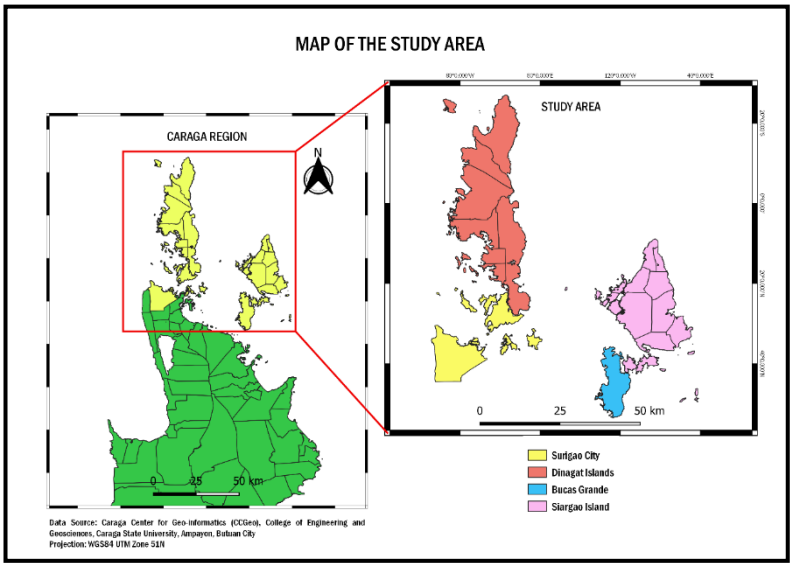

Figure 1. Map of the study area

2. METHODOLOGY

2.1 Coherence Change Image Generation Through Coherence Change Detection

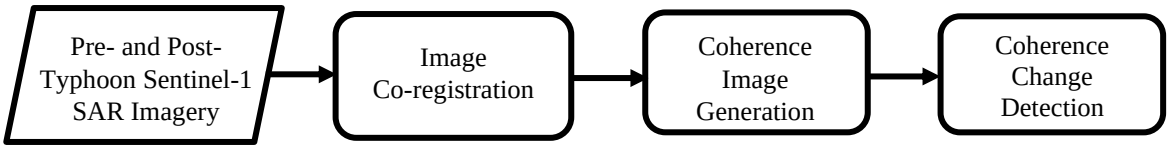

Figure 2. Flowchart for the generation of a Coherence Change Image through Coherence Change Detection

Sentinel-1 SAR SLC imagery acquired on the dates December 2, 14, and 20, 2021, were used for this study. SLC allows the examination of complex coherence, which is suitable for determining small changes between two images that are very close together in time. The SAR images downloaded for change monitoring met the conditions: the same sensor, the same track, the same incident angle, and the same descending pass. To determine the phase difference between the acquisitions, they were co-registered using the back-geocoding operator in SNAP software which co-registered the images using a digital elevation model. Coherence estimation was then done for both pre-disaster and post-disaster co-registered stacks to compute how coherent the pixels between the master and slave images are, which values range from 0 to 1, where 0 means not coherent, and 1 means coherent. Before the generated coherence images could undergo change detection, a multi-look operator and terrain correction operator was applied to reduce speckle noise and remove geometric distortions such as foreshortening, layover, and shadows. The terrain-corrected coherence images for each study area were then stacked to create a single layer containing the two coherence bands, which allowed the use of the change detection operator in SNAP to quantify the change in coherence between the coherence images. This operator calculated a coherence change index, ρ , as the ratio of the coherence estimated for an interferogram that did not cover the typhoon's duration, γ_{pre}, and an image that did, γ_{post} , using the formula:

$$\rho = \frac{\gamma_{pre}}{\gamma_{post}}$$

After generating the coherence change images, the vegetation area was extracted using the ESRI 2021 LULC map to limit the quantification of change in coherence only in vegetation areas.

2.2 NDVI Image Generation

For this study, the NDVI technique was used to determine the changes in vegetation greenness between pre-typhoon and post-typhoon. The datasets used to generate NDVI images were Landsat 8 and 9 Collection 2 Level 2. Since most of the images obtained within the period were greatly covered with clouds, the images that contained even the littlest of usable data were selected and used. Four images were mosaicked for the pre-typhoon and five images for the post-typhoon. Before mosaicking, the images underwent cloud removal to maintain spectral comparability and consistency. Only bands 4 and 5 of the images were used since the formula for NDVI is (NIR – Red)/(NIR + Red), where NIR is the near-infrared reflectance, and Red is the red reflectance (Bolanio et al., 2015). On a pixel-to-pixel basis, the value of the NIR band was subtracted by the value of the red band and was divided by their sum. The output

was a raster file of the NDVI indices ranging from -1 to +1. Higher values of NDVI indicate healthier/greener vegetation, while lower values indicate less or no vegetation.

3. RESULTS AND DISCUSSION

3.1 Coherence Response of Vegetated Areas

The whole vegetation areas were extracted from the coherence images using ESRI's 2021 land use/land cover map. This was done since the researchers were only interested in quantifying changes within vegetation. Additionally, specific vegetation covers, namely trees, grass/shrubs, crops, and flooded vegetation, were extracted from the coherence images using the same land use/land cover map.

This section presents the results of an analysis of averaging the coherence values of the vegetation area of the four study sites to detect the extent of coherence loss using the change percentage formula:

$$A = \frac{\overline{\gamma}_{pre} - \overline{\gamma}_{post}}{\overline{\gamma}_{post}} * 100\%$$

where A is the percentage of change, $\overline{\gamma}_{pre}$, is the mean coherence for the coherence image before the typhoon, and $\overline{\gamma}_{post}$ is the mean coherence for the coherence image spanning the typhoon. Coherence matching was done to ensure that the coherence loss was distributed uniformly in both temporal directions. This was done by selecting the image in the middle of the stack (December 14) as the master for both the coherence images.

Thresholding was done to improve the visual impression of the generated Coherence Images so that they can be easily interpreted. While urban areas are easily detectable, showing high coherence values above 0.6, vegetation areas are dark and have low coherence below 0.3 (Braun and Veci, 2021). To sort out the pixels into change and no change areas, Jenks' Normal Distribution with two classes was first employed using GIS environment for each of the eight images, which gave the researchers a good baseline to find a common threshold between all images that can fairly show the changes. The majority of the values of the pixels ranged from 0 to 0.3, wherein the Jenks' Normal Distribution classified pixels with values 0 to 0.14 in other images and 0 to 0.16 in other images as change, which is the reason why the researchers selected 0.15 as the common threshold through trial and error. In this study, pixels with coherence 0.15 and below are classified as change, and pixels with coherence 0.15 above are classified as no change.

3.1.1 Vegetation per Study Area

The results generally exhibit a loss of coherence when comparing the pre-typhoon coherence images with the post-typhoon coherence images. However, even in the coherence image pre-typhoon, it can be seen that the vegetation cover seems to be experiencing coherence loss in multiple parts of the study area. This can be attributed to the length of the longer temporal baseline (12 days) compared to the shorter temporal baseline (6 days) of the post-typhoon coherence image since vegetation has a short temporal decorrelation due to its dynamic nature.

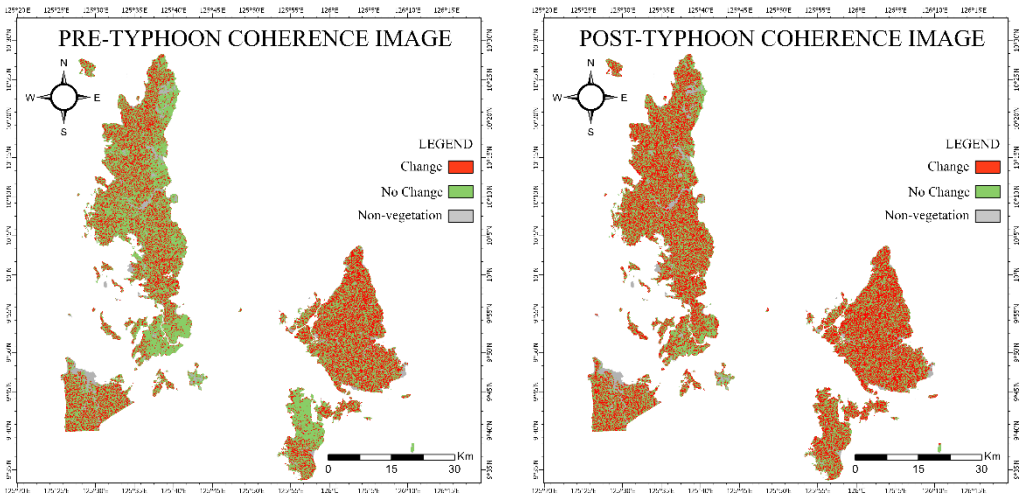

Figure 3. Study area vegetation coherence image classified into change and no-change showing period before the typhoon (December 2, 14, left) and spanning the typhoon (December 14, 20, right)

Bucas Grande exhibited the most vegetation coherence loss out of the four study areas, as observable in Figure 3. Compared to the pre-typhoon vegetation coherence, the post-typhoon vegetation coherence is 46.07% more decorrelated. However, the southern part of the island also seemed to experience coherence loss in both the pre-typhoon and post-typhoon coherence maps. This is followed by Dinagat islands, which experienced 25.12% coherence loss; Surigao City, which experienced 19.14% coherence loss; and Siargao Islands, which only experienced 7.54% coherence loss. This was due to the high coherence loss in the island even in the pre-typhoon coherence image, which can be attributed to external factors causing the vegetations in the study area to move differently during the acquisitions, thus being decorrelated.

3.1.2 Coherence response of different vegetation classes

ESRI's 2021 LULC map was used for further analysis to get an idea of how Typhoon Rai affected each vegetation classification, namely Trees, Grass/Shrubs, Crops, and Flooded Vegetation. In the study area, areas classified as grass/shrubs showed the highest coherence compared to areas classified as trees, crops, and flooded vegetation (Figure 4).

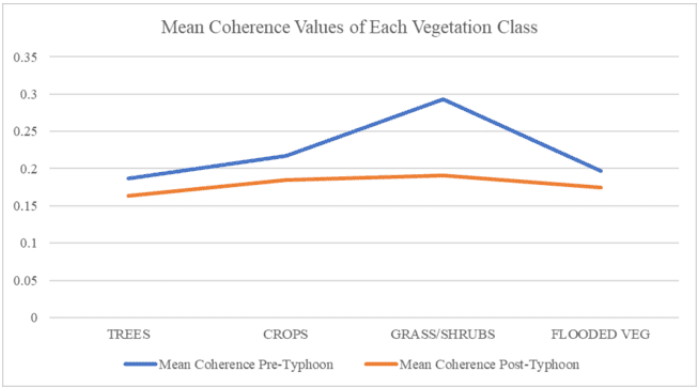

Figure 4. Comparison of mean coherence value of each vegetation land cover type for the pre-typhoon and post-typhoon coherence images.

The tree cover makes up most of the vegetation cover in the study area, covering approximately 77.78%, but only exhibited 14.12% coherence loss. Crops, mainly rice, and corn, comprised 4.3% of the study area and exhibited a 17% coherence loss. Flooded vegetation makes up the least of the vegetation, covering only 2.84%, exhibiting a loss in the coherence of 13.15 %. Of the four vegetation cover types, grass and shrubs exhibited the most extensive coherence loss reaching up to 54.24%. This is also why Bucas Grande exhibited the largest coherence loss among the study areas since most of its land cover is grass and shrubs.

3.2 Coherence Change Image

A coherence change image was generated for each of the study areas. To visualize the extent of change of the coherence change detected images, the ratio of coherence (ρ) table from Hoffmann (2007) was used. This allowed the researchers to classify the areas as severely changed, significantly changed, slightly changed, and no change.

Table 1. Hoffman's change class definition

Coherence Index Range	Classification
$\rho < 1.5$	No Change
$1.5 \leq \rho < 2.0$	Slight Change
$2.0 \leq \rho < 2.5$	Significantly Changed
$\rho \geq 2.5$	Severely Changed

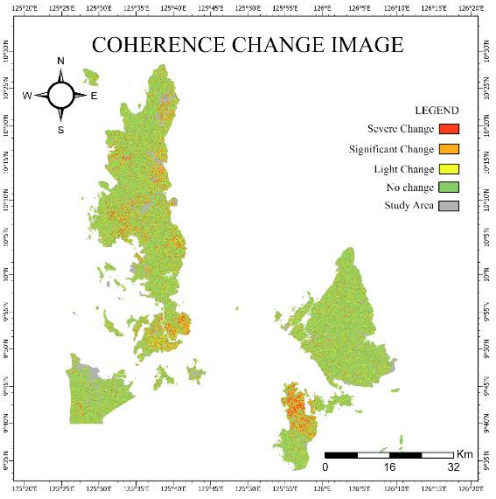

Figure 5. Coherence Change Image of the whole study area

Shown in Figure 5 is the Coherence Change Image of the whole study area, where red pixels are depicted as severe change with a ratio of coherence value equal to or greater than 2.5, and orange pixels represent significant change with ratio values ranging from 2 to 2.5, yellow pixels represent light changes with ratio values ranging from 1.5 to 2, and green pixels represent no changes with ratio values less than 1.5.

3.3 NDVI Image for Pre- and Post- typhoon

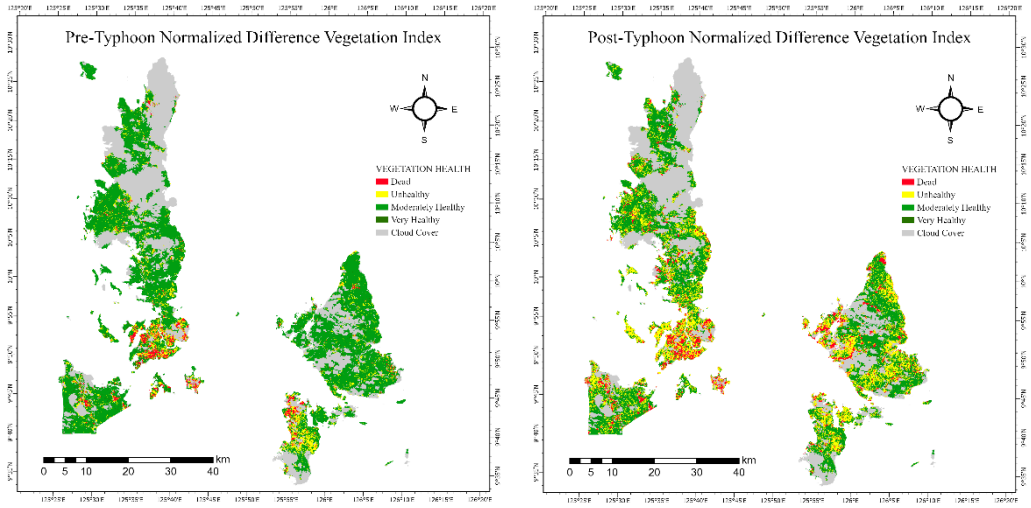

Figure 6. NDVI images for pre-typhoon (left) and post-typhoon

Table 2. NDVI indices classification

Classes	Upper Value	Label
1	≤ 0.2	Dead
2	≤ 0.3	Unhealthy
3	≤ 0.5	Moderately Healthy
4	≤ 1.0	Very Healthy

Shown in Figure 6 are the resulting images from the generation of NDVI for pre-typhoon and post-typhoon. Since the collected images from October 1, 2021, to March 31, 2022, are greatly covered with clouds, the generated mosaics lack some vegetation information. The majority of this can be observed in the Dinagat Islands and some in the other parts of the study area.

NDVI images with DN values that range from -1 to 0.2 are considered non-vegetated areas. Considering that the boundary layer from ESRI's 2021 LULC map represents the vegetated land, those with values -1 to 0.2 may have

been dead or no longer vegetated. The pixel with values ranging from 0.2 to 1 are considered vegetation. The classification for vegetation plant health indication varies from study to study (Anjali and Patil, 2021), (Berhanu and Bisrat, 2018), (Bid, 2016).

To effectively show the different vegetation health conditions, the researchers identified different classes of NDVI values with corresponding health indications, as shown in Table 2. Pixel values ranging -1 to 0.2 are considered dead vegetation. Pixel values ranging from 0.2 to 0.3 are considered unhealthy vegetation. Pixel values ranging from 0.3 to 0.5 are considered moderately healthy vegetation (Bid, 2016). Lastly, pixel values ranging from 0.5 to 1 are considered very healthy (Anjali & Patil, 2021).

It can be gleaned from the pair of images that there are significant changes in NDVI values. Some healthy vegetation in the pre-typhoon NDVI, represented by green-colored pixels, became unhealthy or dead, represented by yellow-colored and red-colored pixels. These changes in NDVI values can be indicative of the damages linked to the typhoon.

3.4 Coherence Change Image Validation

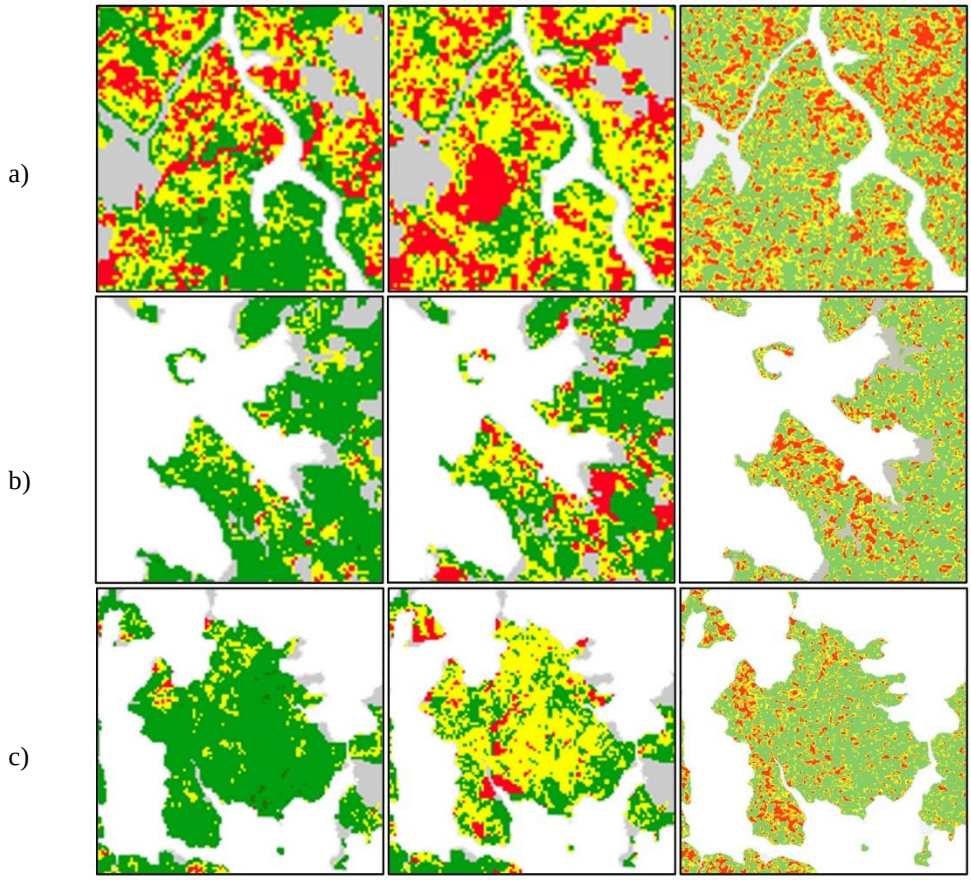

Figure 7. Damage assessment map at parts of Surigao City and Dinagat Islands (row a) Dinagat Islands (row b) and Siargao Islands (row c). Images on the left is the pre-typhoon NDVI and show the situation prior to Typhoon Rai. Images at the middle is the post-typhoon NDVI and show the situation after the typhoon. Images on the right show the damaged areas as estimated using CCD. Red indicates severely damaged; orange means significant damage; while yellow means light damage estimates.

Sample preliminary damage assessments are shown in Figure 21 for three study areas. It can be seen that the change and damage assessment using Sentinel 1 was able to capture certain damaged vegetation cover in Dinagat Islands, Surigao City, and Siargao Islands, as validated quantitively using the generated NDVI images using pre- and post-Landsat images of the study area.

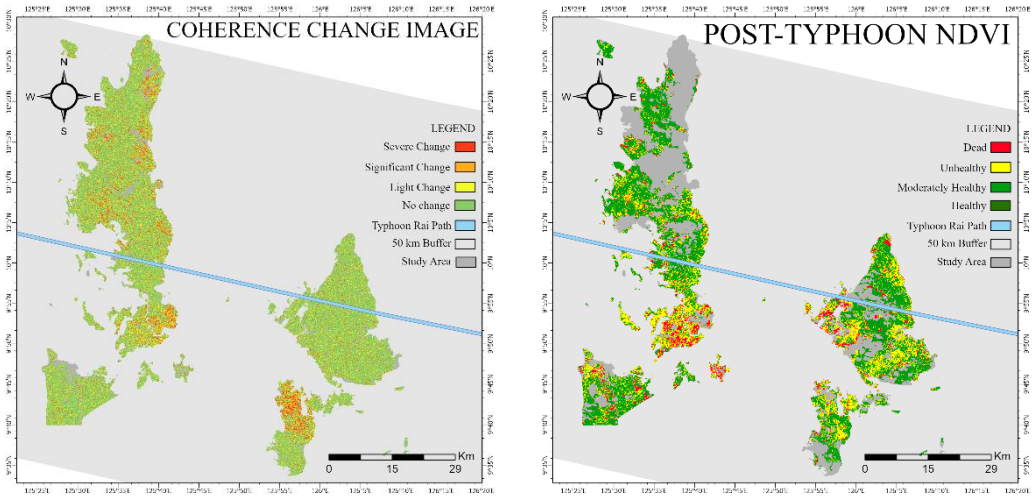

Figure 8. Coherence change image (left) and post-typhoon NDVI image (right) with Typhoon Rai path and buffer zone

Figures 8 shows both the Coherence Change Image and Post-typhoon NDVI image plotted with the typhoon path. It can be observed that the severely changed areas are along and close to the typhoon path. This pattern is an indication that the changes are brought by Typhoon Rai which can be considered as damages.

By correlating the NDVI change image values with the CCD ratio values, the correlation of determination coefficient (R^2) between the two was found to be 0.058. Thus, this means that the two variables are not correlated, wherein no linear relationship exists between them. However, this does not invalidate the association between the CCD and NDVI change values. According to Altman and Krzywinski (2015), association does not always imply correlation.

4. CONCLUSIONS AND RECOMMENDATIONS

4.1 Conclusions

Generating coherence change images as a means to assess vegetation damages is difficult due to its low coherence properties and its short temporal decorrelation, thus, not commonly used. Although this is the case, this study has demonstrated the capability of complex SAR imagery of Sentinel-1 in providing information for post-disaster monitoring in vegetation. Unlike other remote sensing systems, Sentinel-1 missions are ideal for monitoring disasters worldwide since they provide continuous and reliable global data. This study generated coherence images wherein a threshold of 0.15 was applied to show areas of change and no change in the vegetation cover. This allowed the comparison of coherence loss after the Typhoon Rai event. The study area that experienced the most coherence loss is Bucas Grande because most of its land cover is grass and shrubs, the most affected land cover type among the rest. In addition, the coherence change image was generated, and Hoffman's threshold was applied in order to show the areas that experience severe coherence loss, significant coherence loss, slight coherence loss, and no coherence loss. To validate whether the changes in the coherence change image were disaster-induced or just temporal decorrelation, NDVI images were generated. It was found that changes in the NDVI images correspond to the changes in the coherence change image.

The researchers found several limitations in this study in terms of coherence change detection, NDVI images, and the correlation between the two:

- There is no single optical image that sufficiently covered the study area that is acquired near the date of the event, both before and after.
- Since the mosaics for pre- and post-typhoon were collected within six months, three months before, and three months after, there was a non-uniformity of values for NDVI. Some areas depicted more regrowth in the vegetation, especially from those optical images acquired during February and March.
- External factors such as wind could have caused decoherence even before the typhoon. This can be observed in Siargao Islands, wherein the pre-typhoon coherence image already exhibited a low coherence, resulting in a low coherence change percentage compared to the post-typhoon coherence image. This can imply that between the dates December 2, 2021, and December 14, 2021, external factors already caused the decoherence.

4.2 Recommendations

It is shown in this study that damage assessment mapping using Sentinel-1 InSAR coherence change images provides indispensable information to end-users. It is worth noting that the result is dependent on the available optical data for validating these changes as damages. In order to enhance the results, the following recommendations are proposed:

- Incorporate other methods using SAR, such as intensity correlation, in future mapping activities as a means to validate the changes.
- Utilize higher spatial resolution optical imagery for the validation of damages and analysis.
- Generate and use a higher accuracy land use/land cover classification map to accurately delineate vegetated areas.

5. ACKNOWLEDGEMENT

This study was conceptualized through the Earth Observation for Damage Assessment: Case Studies of Typhoon Odette 2021 (EO4D) research project. The researchers would like to acknowledge the Caraga Center for Geo-informatics (CCGeo) for the myriad of datasets utilized in this study.

6. REFERENCES

Altman, N., Krzywinski, M. (2015). Association, correlation and causation. *Nature Methods*, *12*(10), 899–900. https://doi.org/10.1038/nmeth.3587

Anjali, K., Patil, K. A. (2021). NDVI: Vegetation Performance Evaluation using RS and GIS. https://www.walshmedicalmedia.com/open-access/ndvi-vegetation-performance-evaluation-using-rs-and-gis.pdf

Berhanu, B., Bisrat, E. (2018). Identification of Surface Water Storing Sites Using Topographic Wetness Index (TWI) and Normalized Difference Vegetation Index (NDVI). *Journal of Natural Resources and Development*, *8*, 91–100. https://doi.org/10.5027/jnrd.v8i0.09

Bid, S. (2016). Change Detection of Vegetation Cover by NDVI Technique on Catchment Area of the Panchet Hill Dam, India. *International Journal of Research in Geography*, *2*(3). https://doi.org/10.20431/2454-8685.0203002

Bolanio, K., Makinano-Santillan, M., Santillan, J., Daguil, R. (2015). Using Normalized Difference Vegetation Index (NDVI) to Assess Vegetation Cover Change in Mining Areas of Tubay, Agusan del Norte. In: *36th Asian Conference on Remote Sensing, Quezon City, Metro Manila, Philippines*.

Braun, A., Veci, L. (2021). Sentinel-1 Toolbox TOPS Interferometry Tutorial. SkyWatch Space Applications Inc.

Dong, Y., Li, Q., Dou, A., Wang, X. (2011). Extracting damages caused by the 2008 Ms 8.0 Wenchuan earthquake from SAR remote sensing data. *Journal of Asian Earth Sciences*, *40*(4), 907–914. https://doi.org/10.1016/j.jseaes.2010.07.009

Hoffmann, J. (2007). Mapping damage during the Bam (Iran) earthquake using interferometric coherence. *International Journal of Remote Sensing*, *28*(6), 1199–1216. https://doi.org/10.1080/01431160600928567